Title

Engineered Electrical Conduction Tract Restores Conduction in Complete Heart Block From In Vitro to In Vivo Proof of Concept

Journal

Journal of the American College of Cardiology, 64(24)

ISSN

0735-1097

Authors

Cingolani, Eugenio
Ionta, Vittoria
Cheng, Ke
et al.

Publication Date

2014-12-01

DOI

10.1016/j.jacc.2014.09.056

Peer reviewed

Published in final edited form as:

J Am Coll Cardiol. 2014 December 23; 64(24): 2575–2585. doi:10.1016/j.jacc.2014.09.056.

Engineered Electrical Conduction Tract Restores Conduction in Complete Heart Block: From In Vitro to In Vivo Proof-of-Concept

Eugenio Cingolani, MD[*], **Vittoria Ionta, PhD**[*,†], **Ke Cheng, PhD**[*], **Alessandro Giacomello, MD, PhD**[†], **Hee Cheol Cho, PhD**[*], and **Eduardo Marbán, MD, PhD**[*]

[*]Cedars-Sinai Heart Institute, Los Angeles, CA

[†]University of Rome “La Sapienza”

Abstract

BACKGROUND—Cardiac electrical conduction delays and blocks cause rhythm disturbances such as complete heart block, which can be fatal. Standard of care relies on electronic devices to restore synchrony artificially. We sought to create a new modality to treat such disorders by engineering electrical conduction tracts designed to propagate electrical impulses.

OBJECTIVES—We sought to create a new approach to treat cardiac conduction disorders using engineered electrical conduction tracts (EECT).

METHODS—Paramagnetic beads were conjugated with an antibody to γ-sarcoglycan, a cardiomyocyte cell-surface antigen, and mixed with freshly-isolated neonatal rat ventricular cardiomyocytes (NRVMs). A magnetic field was used to pattern a linear EECT.

RESULTS—In an in vitro model of conduction block, EECT, patterned so as to connect 2 independently beating NRVM monolayers, achieved coordinated electrical activity, with action potentials propagating from 1 region to the other via EECT. Spiking EECT with heart-derived stromal cells yielded stable structures with highly reproducible conduction velocities. Transplantation of EECT in vivo restored atrio-ventricular conduction in a rat model of complete heart block.

CONCLUSIONS—A tissue-engineered electrical conduction tract can re-establish electrical conduction in the heart. This novel approach could, in principle, be used, not only to treat cardiac arrhythmias, but also to repair other organs.

Keywords

Arrhythmias; Cardiac Tissue Engineering; Gap Junctions; Heart Conduction System

Correspondence to: Eduardo Marbán, MD, PhD, Cedars-Sinai Heart Institute, 8700 Beverly Blvd. Davis 1090, Los Angeles, CA 90048, Eduardo.Marban@cshs.org. Hee Cheol Cho, PhD, Departments of Biomedical Engineering and Pediatrics, Emory University, 1760 Haygood Dr., HSRB E-184, Atlanta, GA 30322, Tel: 404-727-6356, HeeCheol.Cho@emory.edu.
Drs. Cingolani and Ionta contributed equally to this work.

Disclosures: The authors have reported that they have no relationships relevant to the contents of this paper to disclose.

Introduction

Cardiac electrical conduction delays and blocks are associated with various rhythm disturbances (1), notably complete heart block (aka 3rd-degree atrioventricular [AV] block), which can be lethal. Conduction delays can also create a substrate for re-entrant arrhythmias such as ventricular tachycardia (2). Current therapies depend on electronic pacemakers in the case of heart block, or ablative therapies targeting strands of slowly-conducting viable myocardium to terminate re-entrant circuits in tachyarrhythmias (3). Both strategies are suboptimal. Electronic pacemakers are associated with multiple risks, including an abnormal ventricular activation pattern clinically associated with a progressive decline in pump function (4,5). Ablation destroys living heart tissue and, in ventricular tachycardia, is associated with significant morbidity and mortality (6–8).

We sought to create a new approach to treat such disorders by engineering electrical conduction tracts designed to bridge or bypass zones of impaired conduction. We report a highly generalizable means to engineer electrical conductions tracts (EECT) using magnetic patterning to orient cells conjugated to paramagnetic microbeads. As proof-of-concept, we demonstrate that EECT can re-establish electrical conduction between disconnected regions of two-dimensional cardiac tissue and in an animal model of complete heart block.

Methods

Formation of cell-targeted paramagnetic beads

Paramagnetic fluorescent microspheres (8 μm diameter, Bangs Laboratories, Fishers, IN) were conjugated with γ-sarcoglycan antibody (200 μg; Santa Cruz Biotechnology, Dallas, TX) or with CD105 antibody (200 μg; R&D Technologies, North Kingstown, RI) using the Polylink Protein Coupling Kit (Bangs Laboratories) as per the manufacturer's instructions. In brief, carboxyl-modified polymer-based microspheres were resuspended in Polylink coupling buffer and activated by addition of 1-ethyl-3-dimethylaminopropyl carbodiimide (EDAC). Covalent binding of the specific antibody to the surface of activated microspheres was achieved by incubating 200 μg of either γ-sarcoglycan or CD105 antibodies at room temperature for 2 h. Antibody-coated microspheres were resuspended in Polylink wash/storage buffer and stored at 4 °C for subsequent experiments.

Cardiomyocyte isolation, culture and conjugation

Neonatal rat ventricular myocytes (NRVMs) were isolated from 1 to 2 day-old pups as described (9). We created a 2-dimensional (2D) conduction block model by plating NRVMs in a culture plate, then scraping along the middle of the monolayer. Complete conduction block was confirmed 24 h after mechanical interruption by verifying asynchronous beating of the 2 independent monolayers. Freshly isolated NRVMs (2×10^6) were incubated in suspension with γ-sarcoglycan antibody-coated paramagnetic microspheres for 4 h at room temperature using a 1:1 ratio of cells to microspheres. The newly formed NRVM-microsphere complexes were subsequently used for EECT construction.

Cardiosphere-derived cell culture and conjugation

Human cardiosphere-derived cells (CDCs) were isolated from heart biopsies and cultured as described (10). CDCs were incubated in suspension with CD105 antibody-coated microspheres for 4 h at room temperature using a 1:1 ratio of cells to microspheres. Newly formed CDC-microsphere complexes were utilized for construction of modified EECT (EECT-C).

Construction of EECT *in situ* with magnetic field

To re-establish conduction between the 2 halves of the interrupted NRVM monolayer, an EECT was created by exposing microsphere-NRVM complexes (2×10^6 cells in a 1:1 ratio of cells to microspheres) to a linear magnetic field aligned perpendicularly to the axis of interruption. After 12 h, the cells were removed from the magnetic field and the culture plate was returned to the incubator (Online Figure 1). To enhance the physical integrity of the EECT, NRVM-microsphere complexes were mixed with CDC-microsphere complexes and plated over a linear magnetic field to create CDC-enriched EECT (EECT-C). For in vivo transplantation, microsphere-NRVM complexes were plated in an ultralow attachment plate (Corning, Tewksbury, MA) then exposed for 12 h in the incubator to a linear magnet placed underneath the plate. Nonadherent EECT were created by exposing microsphere-NRVM complexes (5×10^6 NRVMs in a 1:1 cell to microsphere ratio) to the magnetic field.

High-resolution optical mapping

Action potential propagations were recorded on a 469-photodiode array system (WuTech Instruments, Gaithersburg, MD) using a voltage-sensitive dye. Cells were incubated with di-4-ANEPPS (50 μM; Invitrogen, Carlsbad, CA) for 2 min at 37°C, followed by dye washout. To prevent motion artifacts, recordings were obtained at room temperature in Ca^{+2}-free Tyrode's solution containing blebbistatin (10 μM; Sigma-Aldrich, St. Louis, MO). Action potential duration (APD) and conduction velocity (CV) across the NRVM monolayers and the EECT were analyzed with Neuroplex software (RedShirt imaging, Decatur, GA).

Immunomicroscopy and confocal microscopy

For immunohistochemistry, EECTs were fixed overnight with 4% paraformaldehyde, permeabilized, and blocked with DAKO protein block solution (DAKO, Carpinteria, CA) containing 1% saponin (Sigma-Aldrich) for 1½ h. Immunostaining was performed with primary antibodies against the following molecules: connexin 43 (rabbit, Abcam, Cambridge, MA; 1:200), sarcomeric α-actinin (mouse, Sigma-Aldrich; 1:400). Nuclear staining was performed with DAPI, and microspheres were identified by their inherent green fluorescence. Incubation of secondary antibodies conjugated to Cy5 (Abcam; 1:400) or Texas Red (Abcam; 1:400) was performed at room temperature. Images were obtained using a confocal microscope (TCS-SP5-X, Leica Microsystems, Wetzlar, Germany).

To demonstrate in vivo structural integration, rats were transplanted with EECT-C transduced prior to EECT-C construction with a green fluorescent protein (GFP)-expressing adenoviral vector (Ad.GFP). Hearts were harvested 72 h after transplantation, washed with PBS, and fixed with 4% paraformaldehyde. After overnight incubation with 15% sucrose,

hearts were preserved in OCT for cryosectioning. Slides were permeabilized and blocked with DAKO protein block solution (DAKO, Carpinteria, CA) for 1½ h. Immunostaining was performed with the following primary antibodies: connexin 43 (rabbit, Abcam; 1:100), sarcomeric α-actinin (mouse, Sigma-Aldrich, St. Louis, MO; 1:100), GFP (goat, Abcam; 1:50). Nuclei were stained with 4′,6-diamidino-2-phenylindole (DAPI), and paramagnetic spheres were identified by their inherent green fluorescence. Incubation with Alexa Fluor 488 donkey anti-goat IgG, Alexa Fluor 568 goat anti-mouse IgG, or Alexa Fluor 647 goat anti-rabbit IgG (Life Technologies; 1:400) secondary antibodies (Life Technologies) at 1:400 was performed at room temperature. Images were obtained using a confocal microscope (TCS-SP5-X, Leica microsystems, Wetzlar, Germany).

Scanning electron microscopy

Scanning electron microscopy was used to visualize morphological details of EECT 3-dimensional (3D) structure. Samples were fixed with 2% glutaraldehyde in 0.1 M sodium cacodylate (pH 7.2) for 1 h, then dehydrated using progressive ethanol concentrations (35%, 50%, 70%, 80%, 95%, and 100%) for 10 min each and dried in hexamethyldisilazane (Sigma-Aldrich). Scaffolds were sputter-coated with gold and images were captured with a LEO-982 scanning electron microscope (LEO Corporation, Oberkochen, Germany).

In vivo transplantation of ECCT-C

Adult Sprague-Dawley rats (~220 g) were anesthetized using isoflurane (4% induction, 1.5% maintenance), intubated, and mechanically ventilated. Left thoracotomy was performed to expose the heart and the AV groove for direct visualization. Upon removal of the pericardium, a pre-formed EECT-C was laid on top of the heart, connecting the epicardial surfaces of the right atrium (RA) and the right ventricle (RV). The proximal and distal ends of the EECT-C were affixed to the right atrium and right ventricle with fibrin glue. No additional pretreatment was performed at the attachment points. After confirming the implanted EECT-C's mechanical stability, the chest was closed. Animals were reanesthetized 3 days later for in vivo surface electrocardiograms (ECGs), followed by euthanasia and heart harvest. Given the rapid turnover of connexins (11,12), the 3-day time point was chosen to allow the EECT-C to be stably engrafted and electrically coupled with the heart, while minimizing rejection of the donor tissue construct. Harvested whole hearts were mounted on a retrograde Langerdorff perfusion system for recording of surface electrograms (EGMs) through epicardial electrodes connected to a digital recording system (ADInstruments, Colorado Springs, CO). Preparations that showed viability and persistent attachment of the EECT-C were used for the analysis. To assess conduction through EECT-C, the AV node was blocked pharmacologically by adding methacholine (10 mg/ml) to the perfusate. To assay AV conduction, the RA or RV was paced through epicardial platinum electrodes connected to an isolated pulse stimulator (A-M systems, Sequim, WA). Animals were subjected to sham operation (no EECT-C) or –EECT-C transplantation. Investigators were not blinded to the group allocation. All animal experiments were performed in compliance with the Cedars-Sinai institutional animal care and use committee guidelines.

Statistical analysis

Statistical significance was calculated using 2-way ANOVA or Student *t*-test when appropriate. Unless otherwise specified, all data are presented as mean ± standard error of the mean. A p value <0.05 was considered statistically significant.

Results

Creation of an EECT

The concept is to form a complex of cardiomyocytes with paramagnetic beads whose surface is covalently conjugated to a cardiomyocyte-specific antibody. Affinity binding of cardiomyocytes to the beads enables patterning of the complex into a defined structure by attracting the beads with a magnetic field. Paramagnetic beads 8 μm in diameter were activated by EDAC, forming covalent bonds between the free carboxyl groups on the beads' surfaces and the amide groups on EDAC (Figure 1A). Primary antibodies were then conjugated to the activated microspheres via peptide bonds between amino-terminal groups of the antibody and carboxyl groups on the microsphere surface (Figure 1A). This antibody-microsphere conjugation step depends on EDAC's catalytic activity; in its absence, nonspecific primary antibody binding to the beads is undetectable (Figure 1B). The microspheres are manufactured to emit green fluorescence for detection under fluorescence microscopy.

An ideal cell substrate for EECT constructs should have high cell-cell electrical coupling within the EECT and at the ends where the EECT contacts the host tissue. Additionally, the cell substrate should be terminally differentiated so that the EECT retains its conduction properties and shape. For proof-of-concept, neonatal rat ventricular myocytes (NRVMs) satisfy these criteria and thus were chosen as the EECT cell substrate. A number of cardiomyocyte cell surface antigens were tested for their ability to bind to NRVMs, including integrins (α and β), cadherins (N, E, and I), connexins (Cx43 and Cx40), and sarcoglycans. Among them, γ-sarcoglycan-conjugated microspheres exhibited the highest binding efficiency and specificity for NRVMs. Sarcoglycans are integral membrane proteins connecting the contractile apparatus to the extracellular matrix (13–15). Placing a linear magnet underneath a suspension of the microsphere-NRVM complex formed an EECT (Figure 2A, B). Within 24 h, EECT demonstrated rhythmic, syncytial contractions (Online Video 1) indicating that cell-cell electrical coupling was established within the spontaneously-active construct (16). Global electrical coupling in the EECT is further evidenced in Figure 2C, which illustrates spontaneous intracellular Ca^{2+} transients measured from a 1-mm^2 area of the EECT.

EECT bridges conduction between two monolayers of NRVMs

In order to test if EECT could relay electrical signals, we created an in vitro model of conduction block by mechanically disrupting the NRVM monolayers so as to create 2independently-beating halves (Figure 3A). In order to re-establish conduction, EECT were formed in situ by placing a magnet perpendicular to the axis of interruption (Figure 3B). Within 1 day of EECT formation, the 2 NRVM islands beat in tandem, and APs propagated from 1 to the other island via EECT with a conduction velocity (CV) of 18 ± 4 cm/s. Action

potential morphology and APD90 were similar in EECT (APD_{90} = 443 ± 5 ms) and the adjacent monolayers (APD_{90} = 439 ± 12 ms, p = ns). NRVMs cultured as monolayers show occasional spontaneous contractions (17), accounting for the irregular beating shown in Figure 3B. In order to control for nonspecific bridging of the 2 NRVM islands, EECT were formed parallel to the axis of monolayer interruption (Figure 3C). No synchronous beating occurred between the 2 NRVM islands, indicating that the bridging of electrical conduction by EECT is specific, occurring only when EECT termini physically contact the disconnected tissues.

Addition of cardiac stromal cells augments cell viability and electrical conduction properties of the EECT

The EECT used in Figure 2 was composed of NRVMs and beads only. Although capable of bridging a conduction gap (Figure 3), the structure was fragile, which gave rise to large standard deviations in EECT conduction velocities. We thus asked if admixing the NRVMs with another cell type might stabilize the structures. Antibody-mediated cell attachment to paramagnetic microspheres allows incorporation of different cell types using cell type-specific antibodies. Cardiosphere-derived cells (CDCs) are $CD105^+$ stromal cells derived from myocardial biopsies (10), which electrically couple to and exert antiapoptotic effects on cardiomyocytes (10,18). Akin to the native heart, in which the majority of total cardiac cells are nonmyocytes and provide structural support (19–21), we reasoned that addition of CDCs might enhance NRVM viability and/or modulate EECT conduction properties.

To this end, CDCs were bound to CD105-conjugated microspheres, and mixed with NRVMs bound to γ-sarcoglycan-conjugated microspheres. Electron micrographs revealed that EECT constructed with either 2% or 10% CDCs (EECT–C2 or EECT –C10, respectively) exhibited substantially more extracellular matrix than EECT (Figure 4A). EECT-C10 demonstrated a high degree of Cx43-mediated gap junction coupling at cell-cell borders (yellow arrowheads, Figure 4B) and higher cell viability (Figure 4C) than EECT. Measurements of conduction velocity (CV) by optical mapping indicated that NRVM-only EECT conduct at a highly variable velocity of 21.9 ± 19 cm/s (mean ± SD, n = 4). Addition of either 2% or 10% CDCs decreased mean CVs (11.1 ± 7 and 8.7 ± 5 cm/s, respectively). This is not surprising, as CDCs can couple to NRVMs and other CDCs via gap junctions (10), but are themselves inexcitable, acting as electrical sinks. More importantly, EECT-2C and EECT -10C exhibited substantially more consistent CV measurements, with almost 3-fold lower standard deviation (Figure 4D). The uniformly lower CVs also render EECT-2C and EECT -10C as favorable AV node surrogates, avoiding complications associated with rapidly-conducting accessory pathways (22). These findings indicate that CDC addition to EECT renders the construct more consistent in structure and function.

EECT-C re-establishes conduction from the atria to the ventricles in a model of complete heart block

We tested the ability of EECT-C to function in the intact heart in a rat model of complete heart block. We sought to first create an accessory tract for conduction between the atria and ventricles using EECT-C, and then to verify that the EECT could sustain conduction upon suppression of the AV node. For these experiments, we constructed EECT-C10 on a mesh of

30 μm pore size, and implanted by affixing 1 end of the mesh onto the right atrium and the other end onto the anterior surface of the right ventricle of the adult rat heart with fibrin glue. Surface electrocardiograms (ECG) of EECT-C10-implanted animals 72 h later showed an increase in QRS interval duration compared to nonimplanted controls (15.8 ± 0.4 ms vs. 12.8 ± 0.3 ms, $p < 0.05$, $n = 3$ each group; Figure 5A). This verifies creation of a functional accessory tract, as in Wolff-Parkinson-White syndrome (23), albeit without accelerated AV conduction (no significant differences in PR interval duration; Figure 5B).

After in vivo ECG recordings, hearts were explanted and perfused retrogradely for recording of surface EGMs ($n = 2$). Infusion of methacholine created complete heart block and slowed the sinus rate (prolongation of A-A interval), leading to sinus arrest (Figure 5C, top panel). To test conduction via the EECT-C10 upon methacholine-induced AV block, the right atrium was paced electrically, leading to faithful 1:1 capture of the ventricles, as demonstrated by the presence of a ventricular EGM (V) following each atrial EGM (A) and the atrial pacing deflection (P) (Figure 5C, bottom panel). To confirm that the recorded conduction was indeed through the EECT, recordings were repeated after mechanical disruption of the implanted EECT. No evidence of ventricular activity was seen after EECT removal (Figure 5D, top panel). Viability of the ventricular myocardium was verified by the ability to capture the ventricle with a pacing electrode (Figure 5D, bottom panel). Taken together, our data demonstrate that EECT can support functional A-V conduction in the intact heart in a model of complete heart block.

In vivo integration of EECT-C through gap junctions

Integration of EECT-C to the recipient myocardium was assessed by immunohistochemistry of EECT-C transplanted hearts. Prior to implantation, EECT-C was transduced with Ad.GFP to distinguish between transplanted cells and recipient myocardium. Images reveal plentiful Cx43 (red) at the boundary between the EECT-C and the epicardium (Figure 6). Taken together, the *in vitro* and *in vivo* functional and immunohistochemistry data support the notion that the functional A-V conduction by EECT-C is mediated by electrical coupling through connexin 43 gap junctions. Nevertheless, we cannot conclusively rule out the alternative possibility that the coupling is at least partly mechanical (24,25).

Discussion

Current therapies for myocardial conduction blocks depend on electronic devices to deliver electrical pulses downstream of the region of block (26). While effective, it would be desirable to restore conduction or bypass areas of slow conduction by regenerating injured myocardium or by implanting artificial conduction tract. As an alternative to devices and ablative therapies, we engineered de novo electrical conduction tracts capable of bridging myocardial regions of slow conduction or conduction block (Central Illustration).

The ability of isolated ventricular myocytes in culture to spontaneously organize into 3D structures has long been recognized (27). Moreover, a number of 3D tissue culture techniques were developed as biological systems for studying cell-cell interactions, electrical coupling, and extracellular matrix interactions (28–30). Various scaffold-based approaches using different polymers have been utilized. The ability of skeletal myoblast-

based tissue constructs to restore AV conduction in the rat heart was first described by Choi et al. (31). Using a silicone cast, the investigators fabricated small tissue constructs made from a myoblast-Matrigel-based solution, which were subsequently transplanted into the rat heart (31,32). In addition, Kirkton and Bursac (33) engineered 3D cardiac tissue cords consisting of NRVMs and gene-modified HEK293 cells. Although the use of transformed HEK293 cells diminished the immediate therapeutic potential of these constructs, gap-junctional modification of HEK293 cells changed the tissue construct's conduction properties in a predictable manner, providing an in vitro platform for studying cardiac conduction properties.

Our approach uses a magnetic field to pattern an EECT composed of paramagnetic microspheres coated with cell-specific antibodies. As we demonstrate with NRVMs and cardiac stromal cells, the flexibility to conjugate microspheres with different antibodies provides a generalizable platform to engineer EECTs with specific electrophysiological and/or structural properties. Affinity binding between paramagnetic beads and ventricular myocytes was mediated by γ-sarcoglycan, a surface antigen robustly expressed on cardiomyocytes, including those of human origin (34,35). Thus, although not tested here, we anticipate that EECTs constructed with human pluripotent stem cell-derived cardiomyocytes would exhibit similar functionality as those constructed with NRVMs. Addition of cardiac stromal cells increased structural integrity of the EECTs and yielded more consistent conduction properties. Our data demonstrate the ability of the 3D tissue structure to restore cardiac electrical conduction in an in vitro model of conduction block and by implanting a pre-formed EECT-C, in vivo followed by in vivo and ex vivo electrophysiological recordings.

Downstream of the atrioventricular node, the cardiac conduction system is electrically insulated, preventing electrical propagation from dissipating laterally into the surrounding myocardium (36,37). Likewise, end-to-end electrical propagation along the run of the EECT without lateral flux would be desirable to maximize signal fidelity and help overcome impedance mismatch. Our data demonstrate that the EECT constructs transplanted in vivo faithfully relayed atrial activation to the ventricle (Figure 5), indicating that lateral "signal loss" was insignificant. Only the terminal ends of the EECT were fibrin-glued to the myocardium; physical adhesions of the EECT elsewhere may form eventually. Complete electrical insulation of EECT may be challenging, as acellular structures such as microtubules can mediate electrical coupling (38). Nonetheless, our approach to tissue patterning with paramagnetism and carefully-chosen cell surface antigens is amenable to creating insulating layers (should such insulation be required) composed of poorly-coupled cells, such as dermal fibroblasts (39) above and beneath the EECTs,. Besides use of fibrin glue, no treatment was performed to attach the EECT onto the epicardial surface. Fibrin glue provides scaffolding for cardiac tissue engraftment (40), promotes angiogenesis (41), and mediates nerve regeneration by providing a favorable matrix microenvironment (42). Since the EECT ends were affixed to the myocardium at the time of surgery, and connexins turn over rapidly (1.5 to 5 h) (11,12), a 3-day window would be sufficient for establishing gap-junctional and/or acellular electrical coupling (38) of the EECT termini to the myocardium. The presence of connexins at the border between the EECT-C and the epicardium 3 days

after EECT-C transplantation in vivo further supports electrical coupling of EECT-C to the host myocardium, although a role for mechanotransduction cannot be excluded (24,25).

Spontaneous contraction of the EECT (Online Movie 1) arises from occasional self-excitability of some NRVMs, driving contraction of the entire construct, as we observed in NRVM monolayers (43). The rate of these occasional contractions is much lower (~100 beats/min) than the sinus rate of the rat (~320 beats/min). Thus, sinus rhythm is expected to entrain spontaneous contraction of the EECT-C upon implantation in vivo. The EECT is optically thin, with no more than ~5 layers of cells in its short axis. While we did not directly examine EETCs' long-term viability, such thin structures are expected to remain viable via soluble gas exchange without dedicated vasculature. Multiple lines of evidence support this notion, for example:, 1) myoglobin-facilitated O_2 diffusion mechanisms suffice to oxygenate the rat myocardium when cellular oxygen falls low (44); and 2) diffusion coefficients of oxygen in muscle fibers (1.1×10^{-4} to 4×10^{-8} cm^2 sec^{-1}) (45,46) suffice to cover the EECT's cross-sectional dimensions. This proof-of-concept study demonstrates that EECT can re-establish cardiac electrical conduction between isolated regions of 2D cardiac tissue, as well as in the whole heart. Delivery and transplantation techniques need to be refined prior to translating this approach to large-animal models. This technology could also be exploited for alternatives to open chest implantation, such as in situ EECT formation using transcutaneous or transesophageal electromagnetic probes to conglomerate tagged cells. The present approach is highly generalizable, offering a novel platform to engineer biocompatible materials for relaying electrical signals. A similar approach could be used, in principle, to bridge interrupted neural circuits in stroke, nerve, or spinal cord injuries.

Limitations and challenges

As electrical conduction propagates along the EECT, it encounters a highly hyperpolarizing, electrical sink at the EECT-ventricular myocardium interface. This is akin to the source-sink mismatch in the sinoatrial node (SAN) surrounded by the hyperpolarizing atrial myocardium. The SAN solves this problem by populating its pacemaker cells with Cx45-expressing fibroblasts, thereby raising the input resistance (47). Similarly, incorporating relatively uncoupled CDCs (10) into EECTs should increase the input resistance, protecting the electrical source carried along the EECT-C10 from dissipation at the ventricular myocardium. Further in vivo studies are warranted to test this notion. The low number of animals for the in vivo proof-of–concept experiments is a limitation of the present study.

The epicardial positioning of EECT here is purposely extravascular. Nevertheless, the paramagnetic microspheres employed in this study were 8 μm in diameter, which may cause issues if released into the circulation. Although unlikely, this complication can be avoided in future constructs, as the present approach is amenable to smaller or biodegradable spheres, which are both available commercially.

Supplementary Material

Refer to Web version on PubMed Central for supplementary material.

Acknowledgments

The Cedars-Sinai Medical Center Board of Governors Heart Stem Cell Center supported this study. NIH-NCATS UCLA-CTSI UL1TR000124 supports Dr. Cingolani. Dr. Cho is supported by grants from the American Heart Association (12SDG9020030) and the NHLBI (1R01HL111646-01A1). Dr. Cheng is supported by grant from American Heart Association (12BGIA12040477).

References

1. Pistolese M, Richichi G, Catalano V, et al. Electrocardiographic aspects of intermittent atrio-ventricular block in the phase of sinus rhythm. Cardiologia Pratica. 1969; 20:125–37. [PubMed: 5794980]
2. Solligard E, Juel IS, Bakkelund K, et al. Gut luminal microdialysis of glycerol as a marker of intestinal ischemic injury and recovery. Crit Care Med. 2005; 33:2278–85. [PubMed: 16215382]
3. Josephson, ME. Clinical cardiac electrophysiology: techniques and interpretations. Philadelphia, PA: Lippincott Williams & Wilkins; 2008.
4. Wilkoff BL, Cook JR, Epstein AE, et al. Dual Chamber and VVI Implantable Defibrillator Trial Investigators. Dual-chamber pacing or ventricular backup pacing in patients with an implantable defibrillator: the Dual Chamber and VVI Implantable Defibrillator (DAVID) Trial. JAMA. 2002; 288:3115–23. [PubMed: 12495391]
5. Sweeney MO, Hellkamp AS, Ellenbogen KA, et al. MOde Selection Trial Investigators. Adverse effect of ventricular pacing on heart failure and atrial fibrillation among patients with normal baseline QRS duration in a clinical trial of pacemaker therapy for sinus node dysfunction. Circulation. 2003; 107:2932–7. [PubMed: 12782566]
6. Stevenson WG, Soejima K. Catheter ablation for ventricular tachycardia. Circulation. 2007; 115:2750–60. [PubMed: 17533195]
7. Sacher F, Tedrow UB, Field ME, et al. Ventricular tachycardia ablation: evolution of patients and procedures over 8 years. Circ Arrhythm Electrophysiol. 2008; 1:153–61. [PubMed: 19808409]
8. Komatsu Y, Daly M, Sacher F, et al. Endocardial ablation to eliminate epicardial arrhythmia substrate in scar-related ventricular tachycardia. J Am Coll Cardiol. 2014; 63:1416–26. [PubMed: 24486269]
9. Sekar RB, Kizana E, Cho HC, et al. IK1 heterogeneity affects genesis and stability of spiral waves in cardiac myocyte monolayers. Circ Res. 2009; 104:355–64. [PubMed: 19122180]
10. Smith RR, Barile L, Cho HC, et al. Regenerative potential of cardiosphere-derived cells expanded from percutaneous endomyocardial biopsy specimens. Circulation. 2007; 115:896–908. [PubMed: 17283259]
11. Fallon RF, Goodenough DA. Five-hour half-life of mouse liver gap-junction protein. J Cell Biol. 1981; 90:521–6. [PubMed: 7287816]
12. Beardslee MA, Laing JG, Beyer EC, et al. Rapid turnover of connexin43 in the adult rat heart. Circ Res. 1998; 83:629–35. [PubMed: 9742058]
13. Heydemann A, McNally EM. Consequences of disrupting the dystrophin-sarcoglycan complex in cardiac and skeletal myopathy. Trends Cardiovasc Med. 2007; 17:55–9. [PubMed: 17292047]
14. Hack AA, Ly CT, Jiang F, et al. Gamma-sarcoglycan deficiency leads to muscle membrane defects and apoptosis independent of dystrophin. J Cell Biol. 1998; 142:1279–87. [PubMed: 9732288]
15. McNally EM, Passos-Bueno MR, Bonnemann CG, et al. Mild and severe muscular dystrophy caused by a single gamma-sarcoglycan mutation. Am J Hum Genet. 1996; 59:1040–7. [PubMed: 8900232]
16. Er F, Larbig R, Ludwig A, et al. Dominant-negative suppression of HCN channels markedly reduces the native pacemaker current I(f) and undermines spontaneous beating of neonatal cardiomyocytes. Circulation. 2003; 107:485–9. [PubMed: 12551875]
17. Kapoor N, Liang W, Marban E, et al. Direct conversion of quiescent cardiomyocytes to pacemaker cells by expression of Tbx18. Nat Biotechnol. 2013; 31:54–62. [PubMed: 23242162]
18. Smith RR, Barile L, Messina E, et al. Stem cells in the heart: what's the buzz all about? Part 2: Arrhythmic risks and clinical studies. Heart Rhythm. 2008; 5:880–7. [PubMed: 18534373]

19. Camelliti P, Green CR, Kohl P. Structural and functional coupling of cardiac myocytes and fibroblasts. Adv Cardiol. 2006; 42:132–49. [PubMed: 16646588]
20. Nag AC. Study of non-muscle cells of the adult mammalian heart: a fine structural analysis and distribution. Cytobios. 1980; 28:41–61. [PubMed: 7428441]
21. Zak R. Development and proliferative capacity of cardiac muscle cells. Circulation research. 1974; 35(suppl II):17–26.
22. Wellens HJ. Should catheter ablation be performed in asymptomatic patients with Wolff-Parkinson-White syndrome? When to perform catheter ablation in asymptomatic patients with a Wolff-Parkinson-White electrocardiogram. Circulation. 2005; 112:2201–7. discussion 2216. [PubMed: 16203931]
23. Tonkin AM, Wagner GS, Gallagher JJ, et al. Initial forces of ventricular depolarization in the Wolff-Parkinson-White Syndrome. Analysis based upon localization of the accessory pathway by epicardial mapping. Circulation. 1975; 52:1030–6. [PubMed: 1182947]
24. Starzl TE, Hermann G, Axtell HK, et al. Failure of Sino-Atrial Nodal Transplantation for the Treatment of Experimental Complete Heart Block in Dogs. J Thorac Cardiovasc Surg. 1963; 46:201–6.
25. Quinn TA, Kohl P. Mechano-sensitivity of cardiac pacemaker function: pathophysiological relevance, experimental implications, and conceptual integration with other mechanisms of rhythmicity. Prog Biophys Mol Biol. 2012; 110:257–68. [PubMed: 23046620]
26. Epstein AE, DiMarco JP, Ellenbogen KA, et al. American College of Cardiology Foundation; American Heart Association Task Force on Practice Guidelines; Heart Rhythm Society. 2012 ACCF/AHA/HRS focused update incorporated into the ACCF/AHA/HRS 2008 guidelines for device-based therapy of cardiac rhythm abnormalities: a report of the American College of Cardiology Foundation/American Heart Association Task Force on Practice Guidelines and the Heart Rhythm Society. J Am Coll Cardiol. 2013; 61:e6–75. [PubMed: 23265327]
27. Halbert SP, Bruderer R, Lin TM. In vitro organization of dissociated rat cardiac cells into beating three-dimensional structures. Journal Exp Med. 1971; 133:677–95. [PubMed: 4926207]
28. Desroches BR, Zhang P, Choi BR, et al. Functional scaffold-free 3-D cardiac microtissues: a novel model for the investigation of heart cells. Am J Physiol Heart Circ Physiol. 2012; 302:H2031–42. [PubMed: 22427522]
29. Radisic M, Park H, Gerecht S, et al. Biomimetic approach to cardiac tissue engineering. Philos Trans R Soc Londo B Biol Sci. 2007; 362:1357–68.
30. Liau B, Zhang D, Bursac N. Functional cardiac tissue engineering. Regen Med. 2012; 7:187–206. [PubMed: 22397609]
31. Choi YH, Stamm C, Hammer PE, et al. Cardiac conduction through engineered tissue. Am J Pathol. 2006; 169:72–85. [PubMed: 16816362]
32. Sill B, Alpatov IV, Pacak CA, et al. Implantation of engineered tissue in the rat heart. J Vis Exp. 2009 Jun 24. pii: 1139. doi: 10.3791/1139
33. Kirkton RD, Bursac N. Engineering biosynthetic excitable tissues from unexcitable cells for electrophysiological and cell therapy studies. Nat Commun. 2011; 2:300. [PubMed: 21556054]
34. Hack AA, Groh ME, McNally EM. Sarcoglycans in muscular dystrophy. Microsc Res Tech. 2000; 48:167–80. [PubMed: 10679964]
35. Wheeler MT, Allikian MJ, Heydemann A, et al. Smooth muscle cell-extrinsic vascular spasm arises from cardiomyocyte degeneration in sarcoglycan-deficient cardiomyopathy. J Clin Invest. 2004; 113:668–75. [PubMed: 14991064]
36. Atkinson A, Inada S, Li J, et al. Anatomical and molecular mapping of the left and right ventricular His-Purkinje conduction networks. J Mol Cell Cardiol. 2011; 51:689–701. [PubMed: 21741388]
37. Wessels A, Markman MW, Vermeulen JL, et al. The development of the atrioventricular junction in the human heart. Circ Res. 1996; 78:110–7. [PubMed: 8603493]
38. Kohl P, Gourdie RG. Fibroblast-myocyte electrotonic coupling: does it occur in native cardiac tissue? J Mol Cell Cardiol. 2014; 70:37–46. [PubMed: 24412581]
39. Kizana E, Ginn SL, Allen DG, et al. Fibroblasts can be genetically modified to produce excitable cells capable of electrical coupling. Circulation. 2005; 111:394–8. [PubMed: 15687125]

40. Christman KL, Fok HH, Sievers RE, et al. Fibrin glue alone and skeletal myoblasts in a fibrin scaffold preserve cardiac function after myocardial infarction. Tissue Eng. 2004; 10:403–9. [PubMed: 15165457]

41. Bach TL, Barsigian C, Chalupowicz DG, et al. VE-Cadherin mediates endothelial cell capillary tube formation in fibrin and collagen gels. Exp Cell Res. 1998; 238:324–34. [PubMed: 9473340]

42. Choi BH, Han SG, Kim SH, et al. Autologous fibrin glue in peripheral nerve regeneration in vivo. Microsurgery. 2005; 25:495–9. [PubMed: 16145682]

43. Kapoor N, Liang W, Marban E, et al. Direct conversion of quiescent cardiomyocytes to pacemaker cells by expression of Tbx18. Nat Biotechnol. 2013; 31:54–62. [PubMed: 23242162]

44. Lin PC, Kreutzer U, Jue T. Myoglobin translational diffusion in rat myocardium and its implication on intracellular oxygen transport. J Physiol. 2007; 578:595–603. [PubMed: 17038435]

45. Krogh A. The rate of diffusion of gases through animal tissues, with some remarks on the coefficient of invasion. J Physiol. 1919; 52:391–408. [PubMed: 16993404]

46. MacDougall JD, McCabe M. Diffusion coefficient of oxygen through tissues. Nature. 1967; 215:1173–4. [PubMed: 6061810]

47. Camelliti P, Green CR, LeGrice I, et al. Fibroblast network in rabbit sinoatrial node: structural and functional identification of homogeneous and heterogeneous cell coupling. Circ Res. 2004; 94:828–35. [PubMed: 14976125]

PERSPECTIVES

Competency in Medical Knowledge

Although electronic pacemakers are presently employed to manage patients with symptomatic bradycardia, engineered electrical conduction tracts (EECTs) could potentially create a substrate for restoring atrioventricular synchrony in those with AV-nodal block.

Translational Outlook

Refined, less invasive delivery methods are needed to enable transplantation of EECT capable of bypassing areas of conduction block, thereby restoring conduction at various levels of the cardiac conduction system and reducing the need for artificial electronic pacemakers.

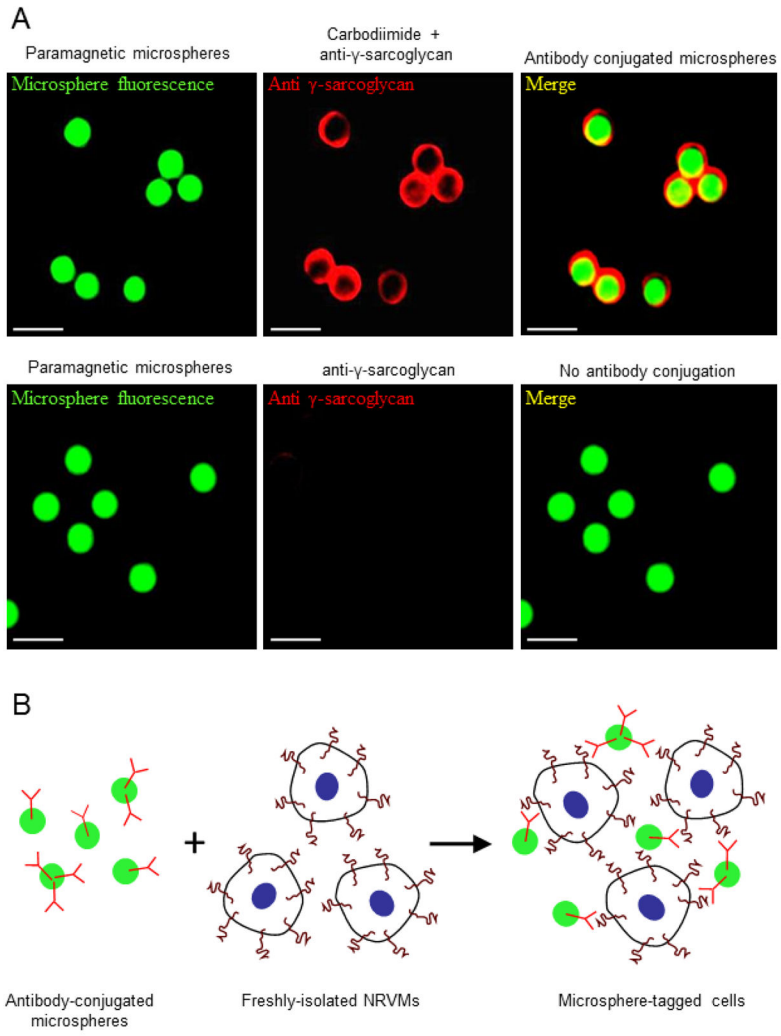

Figure 1. Paramagnetic Bead Conjugation With Cell-Specific Antibodies

Conjugation of green fluorescent microspheres with γ-sarcoglycan antibody (red fluorescence) after activation of the beads' surface carboxyl groups by carbodiimide (EDAC) **(A,** top**)**. In the absence of EDAC, no antibody conjugation was seen **(A,** bottom**).** **(B)** Schematic representation of conjugation of NRVMs with γ-sarcoglycan antibody coated microspheres.

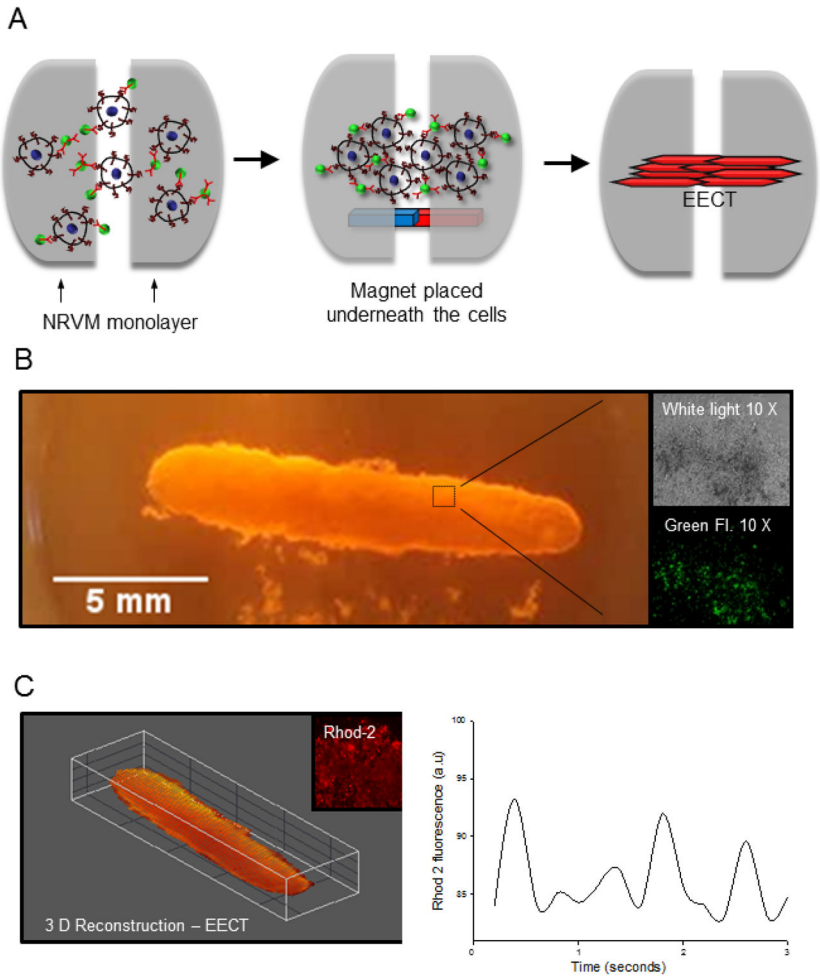

Figure 2. EECT Generation With NRVMs and Paramagnetic Microspheres

(A) Schematic representation of experimental design used to create an EECT to bridge interrupted NRVM monolayers. **(B)** Macroscopic image of EECT in suspension with transmitted light (10X) and green fluorescence (10×) images. **(C)** 3D reconstruction of EECT exhibiting spontaneous whole-cell calcium transients, revealed with the Ca^{2+}-sensitive dye, Ca-Rhod-2. EECT formation was reproduced 20 times from 7 independent NRVM isolations (2 litters per isolation).

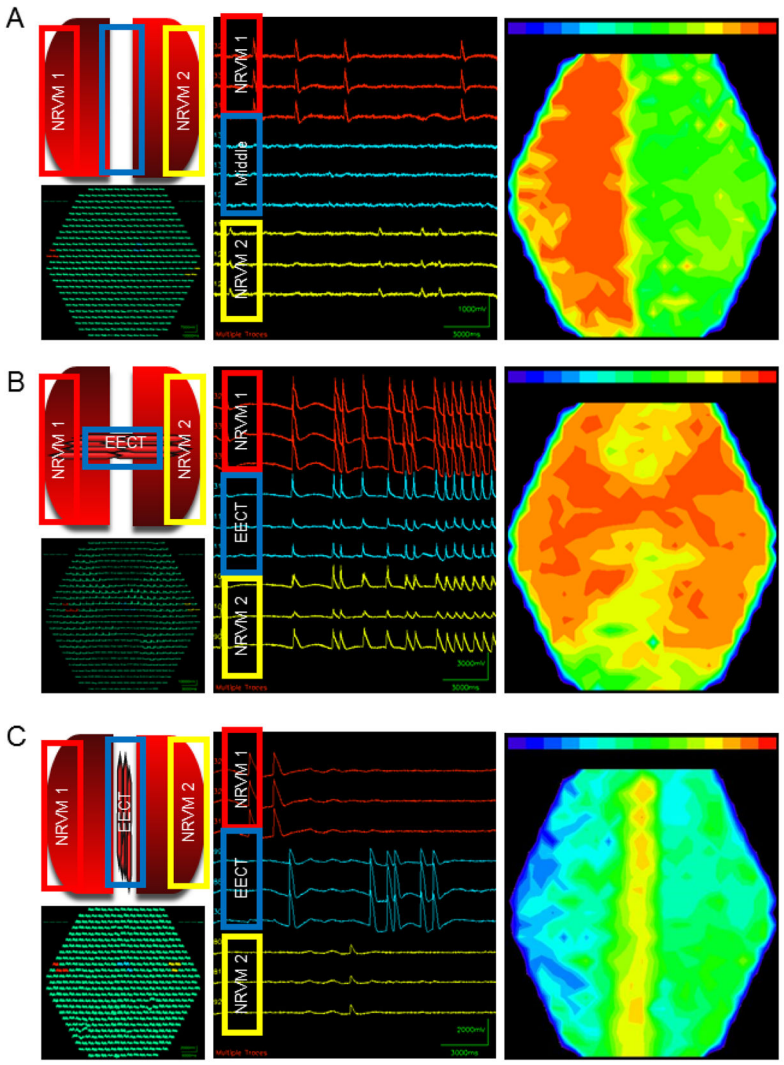

Figure 3. Restoration of Conduction in a 2D Model Of Conduction Block

(A) Optical mapping recordings demonstrate independent activation of interrupted NRVMs monolayer. **(B)** Restoration of conduction block with simultaneous activation of the two NRVM monolayers after EECT implantation. **(C)** Implantation of EECT parallel to NRVM monolayers results in asynchronous activation of the 2 NRVM monolayers. Experiments were reproduced 4 times from 3 independent NRVM isolation procedures (2 litters per isolation).

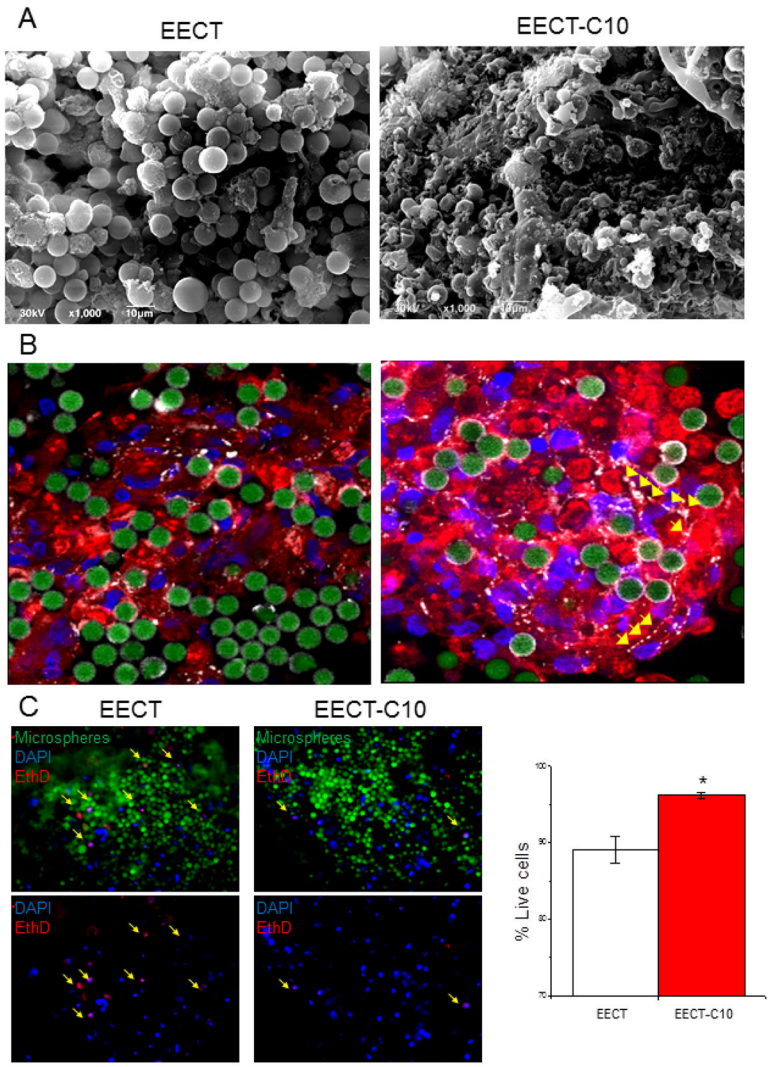

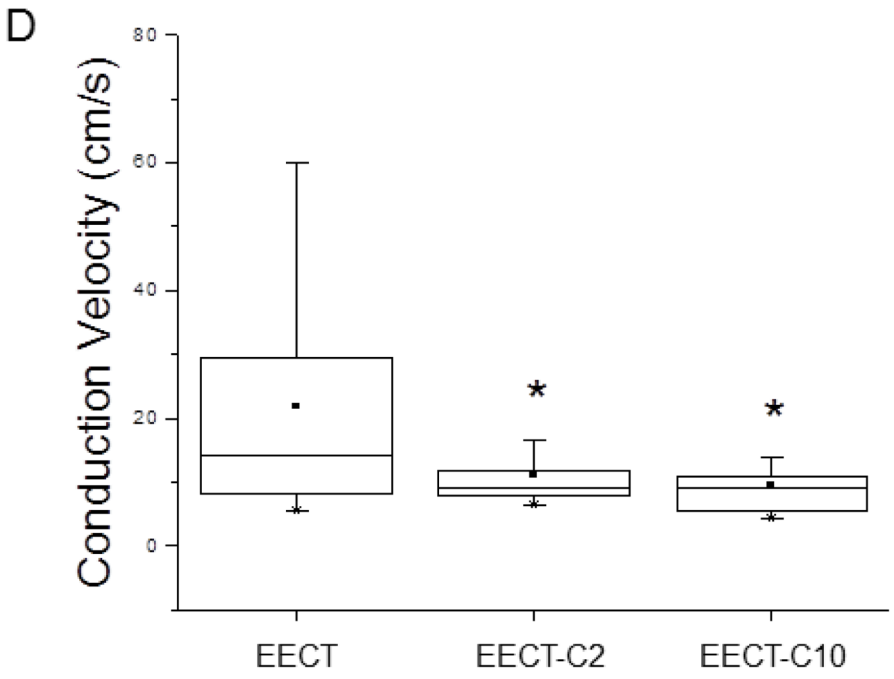

Figure 4. Addition of 10% CDCs to EECT (EECT-C10) Enhances Structural Integrity and Improves Viability of EECT in Culture

(A) Electron microscopy images of EECT (left) and EECT-C10 (right). (B) Immunohistochemistry of EECT (left) and EECT-C10 (right). Green: microspheres, red: sarcomeric actin, white: connexin 43, blue (DAPI): nuclei. Representative images of ethidium homodimer staining of EECT and EECT-C10 **(C**, left**)** and quantification of percent live cells **(C**, right**). (D)** Addition of CDCs to EECT results in less variability in conduction velocity. In each experimental group, n = 3 biological replicates. Error bars represent standard deviation, (*) indicates $p < 0.05$ by 2-way ANOVA.

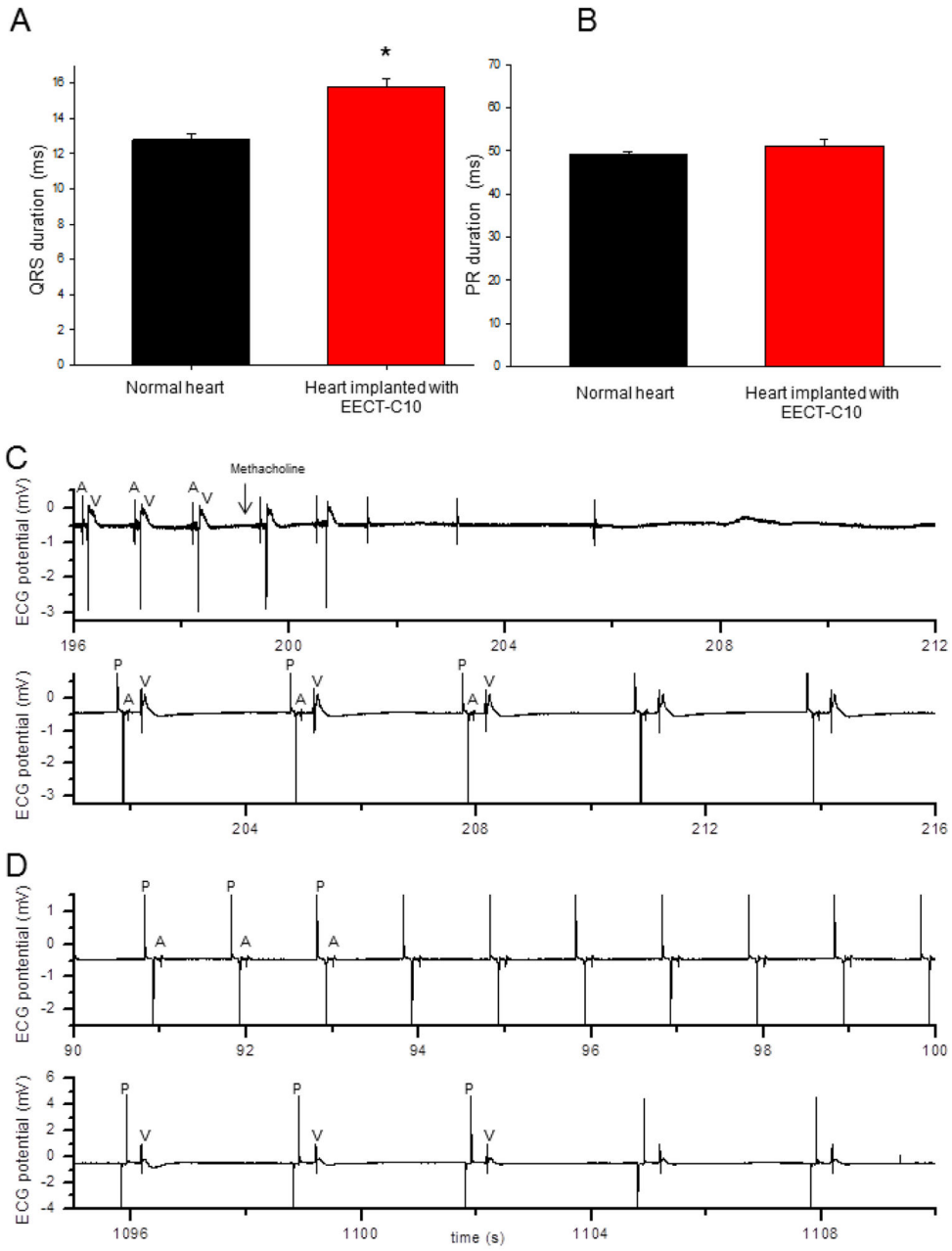

Figure 5. Restoration of AV block By In Vivo Implantation of EECT

QRS interval duration **(A)** and PR interval duration **(B)** in EECT-C10 implanted animals compared to controls. Bars represent mean ± standard error of the mean, n = 3 animals per experimental group. Asterisk (*) indicates p <0.05 by 2-sided Student *t*-test. Electrogram (EGM) recordings of an EECT-C10 implanted heart both pre-infusion and post-methacholine infusion **(C**, top panel**),** and with atrial pacing during methacholine infusion, showing AV conduction **(C**, bottom panel**)**. Recording during mechanical removal of EECT shows pacing deflection (P) followed by atrial depolarization (A) and no ventricular depolarization **(D**, top panel**)**. Recording during ventricular pacing (P) confirms ventricular depolarization (V) confirming viability of the ventricular myocardium **(D**, bottom panel**)**.

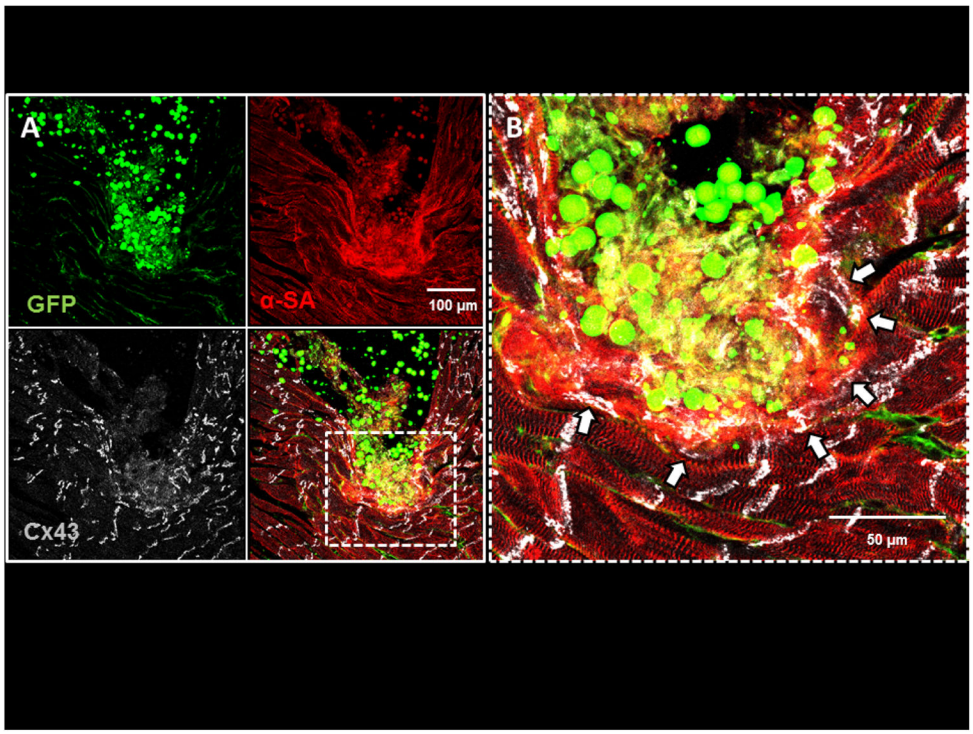

Figure 6. EECT-C Integration With the Recipient Myocardium

Immunohistochemistry of rat myocardium transplanted with EECT-C demonstrates connexin 43 (Cx43)-mediated gap junctions between the recipient myocardium and EECT-C. **(A)** Green: paramagnetic microspheres, manufactured to be green fluorescent, as well as NRVMs and CDCs transduced with Ad.GFP prior to implantation, gray: Cx43, red: sarcomeric α-actinin. Bottom right: merged image of GFP, sarcomeric α-actinin and Cx43. **(B)** Enlargement, demonstrating the presence of Cx43 (white arrows) between EECT-C and the recipient myocardium.

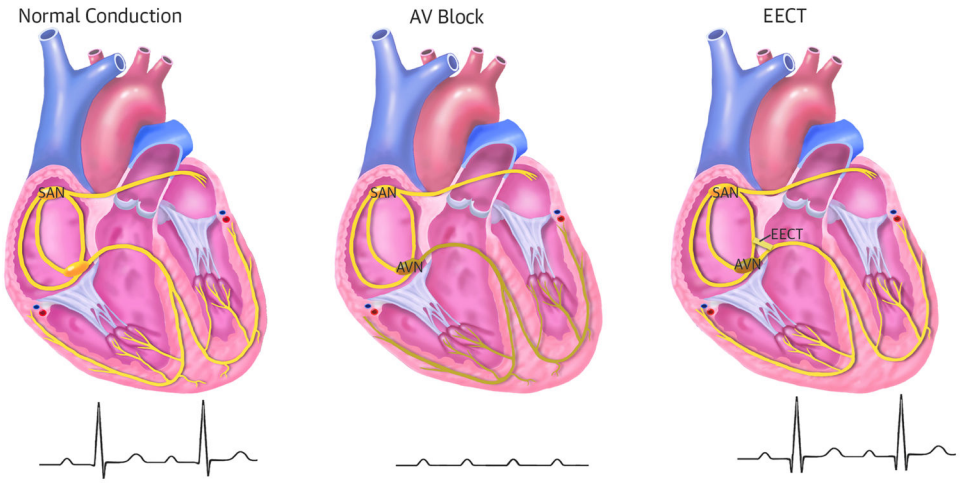

Central Illustration.